Feature Selection Based on Synchronization Analysis for Multiple fMRI Data

Ngoc Dung Bui[1], Hieu Cuong Nguyen[1(✉)], Sellappan Palaniappan[2], and Siew Ann Cheong[3]

[1] University of Transport and Communications, Hanoi, Vietnam
dnbui@utc.edu.vn, cuonggt@gmail.com
[2] Malaysia University of Science and Technology, Petaling Jaya, Selangor, Malaysia
sell@must.edu.my
[3] Nanyang Technologycal University, Singapore, Singapore
cheongsa@ntu.edu.sg

Abstract. Functional magnetic resonance imaging (fMRI) can be used to predict the states of the human brain. However, solving the learning problem in multi-subjects is difficult, because of the inter-subject variability. In this paper, we use the synchronization of fMRI voxels when the brain responds to a stimulus in order to construct features for achieving better data representation and more efficient classification. With a simple definition of synchronization, the proposed method is insensitive to the reasonable choices over a broad range of thresholds. We also demonstrate a new unbiased method to compare multiple subjects by applying the singular value decomposition (SVD) to the discrimination matrix, which enumerates the different patterns. The method for analyzing the fMRI data works well for identifying the meaningful functional differences between subjects.

Keywords: fMRI · Synchronization · SVD

1 Introduction

Functional magnetic resonance imaging (fMRI) is a powerful tool to study the brain activity. The common method to analyze fMRI data is to find non-zero blood oxygen level dependent (BOLD) signal in a large cross section of voxels and apply statistical parametric models to create images of brain activation [1]. Recently, using patterns of the brain activity measured by fMRI data to predict the cognitive states of the subject have been receiving much attention of the neuroscience community [2, 3]. In this approach, one expects brain activation patterns to largely similar for lower-level brain functions, such as vision or motor responses in order to find a common activity model. Thereafter, all subjects are spatially normalized to a common template for creating the voxel correspondence [4]. However, empirical evidence reveals that the activation varies strongly from subject to subject [5, 6] and from group to group [7]. Therefore, simply normalizing data across subjects and pooling the normalized data into region of interest (ROI) super-voxels might not be the best option [8]. We believe that averaging multiple fMRI time series should only be performed after we understand the sources of variations in the data.

N.T. Nguyen et al. (Eds.): ACIIDS 2016, Part I, LNAI 9621, pp. 679–687, 2016.
DOI: 10.1007/978-3-662-49381-6_65

When analyzing multiple subjects, a widely used method is to average data across subjects in the same task [8, 9]. However, for an inhomogeneous group of subjects, this method gives incorrect description of subject-to-subject variation. Most fMRI studies do not concentrate on diagnostic classification and utilize group averaging in order to differentiate subject classes, such as age or clinical conditions. Moreover, since the group-averaged activation profiles cannot be used for a high demanding problem of classification, there is simply no prediction accuracy. When a fMRI dataset becomes larger, the classification will be more severe, because some manually curated classifiers can be statistically meaningful, but other classifiers cannot. In general, these meaningful classifiers are not known beforehand. Thus, there is a need to develop automatic classification algorithms that can exploit the ever-growing of fMRI dataset for knowledge discovery.

The structure of the rest of this paper is as follows. In Sect. 2, we describe the synchronization method for analysis of the fMRI data and show how the synchronization patterns were constructed. Section 3 presents experimental results of the proposed method. Finally, we conclude the paper in Sect. 4.

2 Proposed Method

2.1 Synchronization Approach

An fMRI signal consists of activated signals and uninterested signals, such as physiology-related or motion-related signals. To extract the activation areas, we employ the independent component analysis (ICA) [10] to a group of Alzheimer's disease and normal subjects which we described in Sect. 3. The sensory-motor experiment suggests that the ROIs are those associated with visual processing and motor response. Next, we created a brain mask consisting of the regions using the Brodmann template. After applying the ICA, an activation map consisting of voxels, whose spatial map of highest correlation was selected. The ROIs which can be identified are the primary motor cortex (PMC), the supplementary motor area (SMA), the primary visual cortex (PVC), and the extrastriate visual cortical areas (EVC) (Fig. 1).

For a particular active region, many voxels must be activated simultaneously in order to make a strong response. This implies that a large cross section of voxels should be synchronized for reaction to a stimulus. These cross sections of voxels can be discovered through statistical clustering that is based on the magnitude of their responses to the experiments [11]. The similarity between voxel time series are commonly measured with linear techniques, such as the coherence [12] and the duration of coupling between a pair of neurophysiological processes [13].

Coherence measures the synchronization in the frequency domain, by comparing the average cross and power spectra of the two time series across the low-frequency band. At the same time, the duration of coupling between a pair of neurophysiological processes is the length of time that their band-pass filtered signals are in phase synchronization with each other. The color maps of the coherence and the duration of coupling between a pair of neurophysiological processes of four Brodmann areas are shown in Fig. 2.

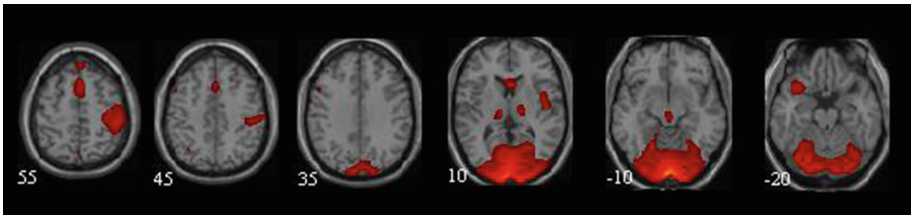

Fig. 1. Slices of the standardized anatomical brain showing the most strongly activated voxels obtained by ICA on the group of 27 subjects, over a brain mask comprising the visual processing and motor response Brodmann areas.

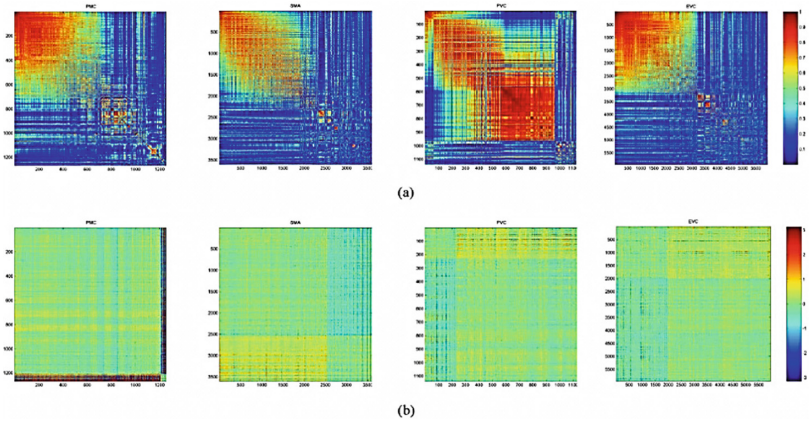

Fig. 2. Color maps of the (a) coherence matrices and (b) phase difference matrices between voxels within (left to right) the primary motor cortex (PMC, 1267 voxels), the supplementary motor area (SMA, 3601 voxels), the primary visual cortex (PVC, 1137 voxels), and the extrastriate visual cortical areas (EVC, 5949 voxels) of Alzheimer subject 2. The average coherences over all voxels over all times are 0.35 ± 0.29 (PMC), 0.32 ± 0.27 (SMA), 0.48 ± 0.31 (PVC), and 0.33 ± 0.29 (EVC). The average phase differences between all voxel pairs over all times are -0.06 ± 0.74 (PMC), 1.3 ± 1.5 (SMA), 0.02 ± 0.55 (PVC), and 0.01 ± 0.52 (EVC).

Although these approaches can measure the synchronization, they have some limitations. First, we have to choose a time window for measuring frequency spectrums. Moreover, no assumption is made for the synchronized cross section, i.e. as long as the synchronization is persistent in time, it can be detected even if only two of K voxels are synchronized. Another method, which applies a grapth theory on resting state fMRI and uses graph measured as features for classification [14]. However, as we mentioned, physiologically meaningful synchronizations present large spatial cross sections. In this paper, we show how one can take advantage of this large spatial cross section of synchronized voxels in order to detect brief synchronizations.

Consider $x_i(t)$ and $x_j(t)$ are the BOLD signals from two voxels i and j. Their standardized fMRI activities can be defined as follows:

$$\zeta_i(t) = \frac{x_i(t) - \frac{1}{N}\sum_{s=1}^{N} x_i(s)}{\sqrt{\frac{1}{N-1}\left[\sum_{s=1}^{N} x_i^2(t) - \left(\frac{1}{N}\sum_{s=1}^{N} x_i(s)\right)^2\right]}},$$

$$\zeta_j(t) = \frac{x_j(t) - \frac{1}{N}\sum_{s=1}^{N} x_j(s)}{\sqrt{\frac{1}{N-1}\left[\sum_{s=1}^{N} x_j^2(t) - \left(\frac{1}{N}\sum_{s=1}^{N} x_j(s)\right)^2\right]}}.$$

The two voxels i and j are instantaneously synchronized if both of the standardized fMRI activities $\zeta_i(t)$ and $\zeta_j(t)$ achieve a given threshold at the same time t. In experiments, this synchronization is robust because it does not depend on a particular selected threshold.

From the standardized fMRI activities, we can calculate the dynamic standard deviation as below:

$$\sigma(t) = \frac{1}{N}\sum_{i=1}^{N} (\zeta_i(t) - \mu(t))^2.$$

This equation gives us a sense of the varying of the BOLD signals across voxels at any given point of time. The dynamic standard deviation is mostly constant except when the episodes of activation are very differential.

To ensure that only stimulation signals were picked up, we considered two voxels as being instantaneously synchronized only if they emerge together from a rejection band. The rejection band in $(-\sigma, +\sigma)$ for the rest of the paper is the time average of the dynamic standard deviation. It can be computed as follows:

$$\sigma = \frac{1}{T}\sum_{t=1}^{T} \sigma(t)$$

Next, we define the positive synchronization and negative synchronization fractions at time t:

$$\rho_+(t) = \frac{1}{N}\sum_{i=1}^{N} \theta(\zeta_i(t) - \sigma),$$

$$\rho_-(t) = \frac{1}{N}\sum_{i=1}^{N} \theta(-\zeta_i(t) - \sigma)$$

where the fractions of voxels whose standardized fMRI signals rise above or fall below $+\sigma$ $(-\sigma)$ and the unit step function can be computed as follows.

$$\theta(x) = \begin{cases} 1, & x > 0; \\ 0, & \text{otherwise} \end{cases}.$$

It is noted that $\rho_+(t)$ and $\rho_-(t)$ represent the spatial cross sections of positive and negative synchronizations.

In Fig. 3, the positive and negative synchronization fractions can be seen on the top and in the middle row. The relative strengths of the positive synchronization peaks coincide with troughs of the negative synchronization. It ensures the synchronization patterns observed are functionally meaningful, or at least as meaningful as the mean time course in measuring cognitive functions. These synchronization patterns in the four ROIs can be better visualized in a single color map (bottom row), where the blue area indicates strong negative synchronization and the red area indicates strong positive synchronization. In this color map, the green area indicates the absence of strong positive or negative synchronizations.

2.2 Feature Selection

We look for the described above differentiated responses in different ROIs in the brain. There are two ways for the responses of different ROIs to be discriminated: (1) synchronizing a ROI before synchronizing another ROI, (2) synchronizing a ROI is stronger than another ROI. In fMRI experiments, it may be difficult to see the first type of differentiation because of low time resolution, so we concentrate on looking for the second type of differentiated response, as shown in Fig. 3.

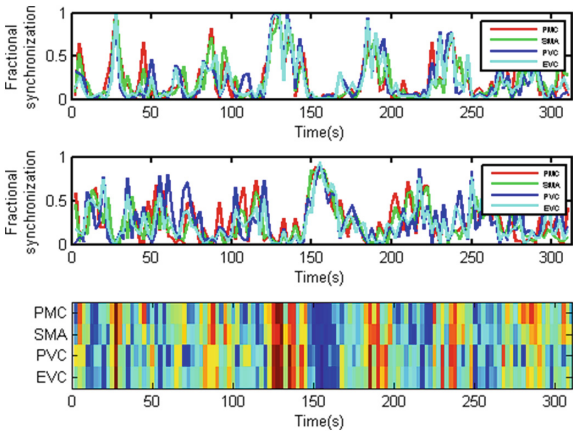

Fig. 3. Positive and negative synchronization patterns of four Brodmann areas: primary motor cortex (PMC) (red), supplementary motor area (SMA) (green), primary visual cortex (PVC) (blue), and extrastriate visual cortical areas (EVC) (cyan) in Alzheimer subject 2 (Color figure online).

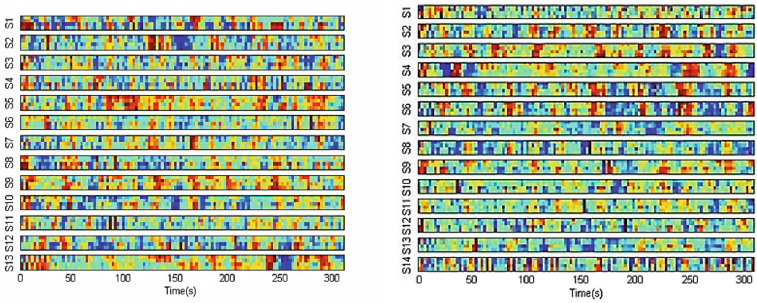

Fig. 4. Synchronization color maps of all ROIs in all 13 Alzheimer and 14 normal subjects

In Fig. 4, we show the synchronization fractions of all ROIs in 13 Alzheimer and 14 normal subjects. If the subjects were given the same task sequence, we would be able to directly compare functional differences in their responses to the tasks. In this figure, the task sequence varies from subject to subject. Therefore, though the synchronization patterns are interesting, the functional responses of different subjects can not be directly compared. For such fMRI data, we must perform functional comparison indirectly between different subjects. To this end, a discrimination matrix has been constructive.

Firstly, we go through the synchronization pattern of an individual subject and find an instance of a particular ordering of synchronization fractions. For example, the strongest synchronization can be found in the PMC, the next strongest synchronization in the SMA, followed by the PVC, and then the EVC areas for a particular stimulation episode. This is a functional pattern we may find in other subjects as well. Thus we search exhausting functional patterns and list the subjects we find these patterns in the form of a non-square matrix. In this discrimination matrix, called D the rows represent different subjects while the columns represent different functional patterns, such that $D_{ij} = 1$ if functional pattern j is found in subject i, and $D_{ij} = 0$ otherwise. After that, we utilize SVD analysis for the matrix D ($D = U\Sigma V^T$), where the columns of U are eigenvectors of subjects and the columns of V are eigenvectors of functional patterns.

3 Experimental Results

3.1 Data Preparation

We used the publicly-known data of Washington University [15]: 13 subjects (six males with the mean age of 77.2 years) with very mild to Alzheimer's Disease conditions and 14 normal subjects (five males with the mean age of 74.9 years) were scanned in a simple sensory-motor experiment. The functional images were obtained using asymmetric spin-echo sequence sensitive to BOLD contrast with following parameters: TR = 2.68 s; 3.75 × 3.75 mm in-plane resolution; T2* evolution time = 50 ms (ms); alpha = 90°. Whole brain volumes were obtained using 16 contiguous 8-mm think slices with parallel to the plane of the anterior-posterior commissure. The raw data were received from the fMRI Data Center at Dartmouth College

and preprocessed using SPM8 [16]. The images were motion corrected and normalized to coordinates of Talairach and Tournoux [17]. They were also smoothed with a 4 mm Gaussian kernel to decrease spatial noise.

3.2 Results

Referring to Fig. 4, we recognized that there is no easy way to directly compare the synchronization patterns of different subjects since the sequences of tasks that given to the subjects are different. Therefore, we constructed a discrimination matrix to look for hidden functional differences between subjects. As we are interested in the functional classification of subjects, we plot the weights of each subject along the first and second principal components of U. Clusters that appear in such a plot give a natural classification scheme (Fig. 5).

Alternatively, if we are interested in a natural classification scheme for the functional patterns, we can plot the weights of each functional pattern along the first and second principal components of V. Again clusters that might appear in such a plot would allow us to naturally classify functional patterns. We found that the Alzheimer and normal subjects are not differentiated, during positive or negative synchronizations. Thus, these two pieces of information in the form of a reordered version of the discrimination matrix can be combined. To reorder the discrimination matrix, we make use of the fact that the second principal component is generally associated with the greatest difference between subjects. In this second principal component, a subject with positive weight has similar functional patterns compared to another subject with positive weight, but dissimilar functional patterns from a subject with negative weight. Therefore, we reordered the subjects, so that those with positive weights come first, followed by those with negative weights.

We combined two pieces of information in the form of the reordered version of the discrimination matrix. In the second principal component, a subject with positive weight has similar functional patterns compared to another subject with positive weight, but

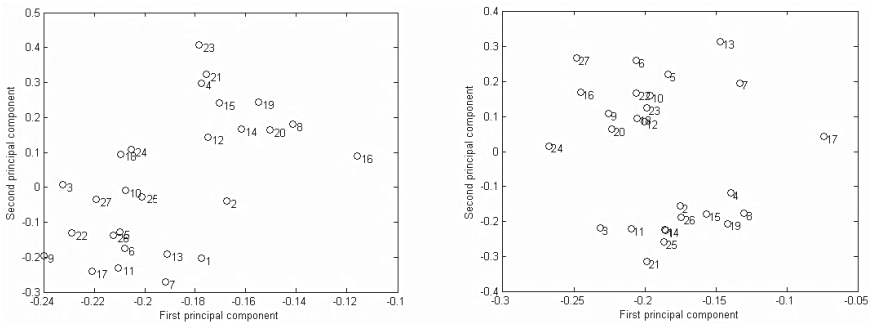

Fig. 5. Plots of weights of individual subjects (27 subjects, including 13 Alzheimer and 14 normal) of the first and second principal components of the discrimination matrices obtained from positive synchronization (left) and negative synchronization (right).

dissimilar functional patterns from a subject with negative weight. From reordered discrimination matrix, we found mostly nondiscriminatory patterns that appear in all subjects. However, we recognized discriminatory patterns and the two clusters of subjects are primarily discriminated by the positive synchronization patterns:

1 (PMC>SMA>PVC>EVC) 7 (PMC>EVC>PVC>SMA)
8 (SMA>PMC>PVC>EVC) 16 (PVC>PMC>EVC>SMA)
18 (PVC>SMA>EVC>PMC) 26 (EVC>PVC>PMC>SMA)
27 (EVC>PVC>SMA>PMC)

From negative reordered matrix, it is shown that the two clusters of subjects are primarily discriminated by the negative synchronization patterns:

1 (PMC>SMA>PVC>EVC) 4 (PMC>PVC>SMA>EVC)
6 (PMC>EVC>SMA>PVC) 7 (PMC>EVC>PVC>SMA)
8 (SMA>PMC>PVC>EVC) 18 (PVC>SMA>EVC>PMC)
19 (PVC>EVC>PMC>SMA) 23 (EVC>SMA>PMC>PVC)
24 (EVC>SMA>PVC>PMC)

Here we found the primary motor cortex (BA4) being most frequently the most negatively synchronized, followed by the primary visual cortex (BA17) and the extrastriate visual cortical area (BA18/BA19).

4 Conclusion

In this paper, we have presented a new and effective feature selection method for analyzing fMRI data to find the meaningful functional differences between subjects. Instead of looking for average activation profiles, we examined synchronization patterns in different parts of the human brain. Based on these patterns we constructed a discrimination matrix between subjects and between synchronization patterns, whose matrix elements tell us whether a given pair of subjects can be discriminated by a given positive or negative synchronization pattern. When subjects can be classified into natural clusters, we showed that it is possible to identify the most important functional differences between these subject clusters.

References

1. Friston, K.J., Jezzard, P., Turner, R.: Analysis of functional MRI time-series. Hum. Brain Mapp. **1**(2), 153–171 (1994)
2. Kenneth, A.N., Sean, M.P., Greg, J.D., James, V.H.: Beyond mind-reading: multi-voxel pattern analysis of fMRI data. TRENDS in Cogn. Sci. **10**(9), 424–430 (2006)
3. Mitchell, T.M., Hutchinson, R., Niculescu, R.S., Pereira, F., Wang, X., Just, M., Newman, S.: Learning to decode cognitive states from brain images. Mach. Learn. **57**, 145–175 (2004)

4. Friston, K.J., Holmes, A.P., Worsley, K.J., Poline, J.B., Frith, C.D., Frackowiak, R.S.J.: Statistical parametric maps in functional imaging: a general linear approach. Hum. Brain Mapp. **2**, 189–210 (1995)
5. Mechelli, A., Penny, W., Price, C., Gitelman, D., Friston, K.: Effective connectivity and inter-subject variability: using a multi-subject network to test differences and commonalities. NeuroImage **17**, 1459–1469 (2002)
6. Smith, S.M., Beckmann, C.F., Ramnani, N., Woolrich, M.W., Bannister, P.R., Jenkinson, M., Matthews, P.M., McGonigle, D.J.: Variability in fMRI- a re-examination of inter-session differences. Hum. Brain Mapp. **24**, 248–257 (2005)
7. Buckner, R.L., Snyder, A.A., Sanders, A.L., Raichle, M.E., Morris, J.C.: Functional brain imaging of young, nondemented, and demented older adult. J. Cogn. Neurosci. **12**, 24–34 (2000)
8. Wang, X., Hutchinson, R., Mitchell, T.M.: Training fMRI classifiers to discriminate cognitive state across multiple human subjects. In: Proceedings of the 18th Annual Conference on Neural Information Processing Systems. Vancouver, Canada (2004)
9. Schmithorst, V.J., Holland, S.K.: Comparison of three methods for generating group statistical inferences from independent component analysis of functional magnetic resonance imaging data. J. Magn. Reson. Imaging **19**, 365–368 (2004)
10. Calhoun, V.D., Adali, T.: Unmixing fMRI with independent component analysis. IEEE Eng. Med. Biol. Mag. **25**, 79–90 (2006)
11. Thirion, B., Faugeras, O.: Feature characterization in fMRI data: the information bottleneck approach. Med. Image Anal. **8**, 403–419 (2004)
12. Liu, D., Yan, C., Ren, J., Yao, L., Kiviniemi, V.J., Zang, Y.: Using coherence to measure regional homogeneity of resting-state fMRI signal. Front. Syst. Neurosci. **4**, 4–24 (2010)
13. Kitzbichler, MG, Smith ML, Christensen, SR, Bullmore E: Broadband criticality of human brain network synchronization. PLoS Computational Biology (2009)
14. Khazaee, A., Ebrahimzadeh, A., Babajani-Feremi, A.: Identifying patients with Alzheimer's disease using resting-state fMRI and graph theory. Clin. Neurophysiol. **126**(11), 2132–2141 (2015)
15. Buckner, R.L., Snyder, A.A., Sanders, A.L., Raichle, M.E., Morris, J.C.: Functional brain imaging of young, nondemented, and demented older adult. J. Cogn. Neurosci. **12**, 24–34 (2000)
16. SPM8, Statistical Parametric Mapping (2008). http://www.fil.ion.ucl.ac.uk/spm/
17. Talairach, J., Tournoux, P.: Co-Planar Stereotaxic Atlas of the Human Brain. Thieme. Stuttgart, Germany (1998)